Bright and highly valley polarized trions in chemically doped monolayer MoS

Zhang, Wenjin; Tanaka, Kenya; Hasegawa, Yusuke; Shinokita, Keisuke; Matsuda, Kazunari; Miyauchi, Yuhei

Applied Physics Express

The Japan Society of Applied Physics

LETTER • OPEN ACCESS

Bright and highly valley polarized trions in chemically doped monolayer MoS_2

To cite this article: Wenjin Zhang *et al* 2020 *Appl. Phys. Express* **13** 035002

Applied Physics Express 13, 035002 (2020) LETTER
https://doi.org/10.35848/1882-0786/ab7485

Bright and highly valley polarized trions in chemically doped monolayer MoS_2

Wenjin Zhang, Kenya Tanaka, Yusuke Hasegawa, Keisuke Shinokita, Kazunari Matsuda, and Yuhei Miyauchi*

Institute of Advanced Energy, Kyoto University, Uji, Kyoto 611-0011, Japan

*E-mail: miyauchi@iae.kyoto-u.ac.jp

Received January 20, 2020; revised February 4, 2020; accepted February 9, 2020; published online February 25, 2020

We demonstrate the effect of *p*-type dopant F_4TCNQ molecular adsorption on the photoluminescence (PL) and valley polarization properties of trions in monolayer (1L) MoS_2 at 15 K using a spatial PL mapping method. Trion PL intensity considerably increased after the treatment, which was attributed to the extended trion nonradiative lifetime (~70 ps). Trion valley polarization as high as 0.75 showed a negligible decrease after the chemical treatment, as is the manifestation of a long trion valley lifetime of more than nanoseconds order. The results suggest that this method will be useful for future optovalleytronics applications of these materials. © 2020 The Japan Society of Applied Physics

Supplementary material for this article is available online

Monolayer (1L) transition metal dichalcogenides (TMDs) show promise for future applications in electronics and optoelectronics beyond graphene because of their finite direct band gaps and readily tunable physical and electrical properties.[1–4] Some 1L TMDs, such as MoS_2 and WSe_2, possess two degenerate valleys, K and K′, at the corners of the hexagonal Brillouin zone. The strong spin–orbit interaction and their broken spatial inversion symmetry enable a mutual conversion between valley polarized excitons/charged excitons (trions) and circularly polarized photons.[5–7] This unique characteristic makes these 1L materials attractive, especially for exploiting valleytronics or optovalleytronics that make use of the valley degree of freedom for fast and energy-saving information processing.[8–10] Previous reports showed that exciton valley polarization can be modulated using a magnetic field,[11–14] photon-upconversion process,[15,16] carrier density,[17–22] and van der Waals engineering.[23–26] However, a short valley lifetime of bright excitons in 1L TMDs has been reported and is considered as a major limitation for the application of valley polarization.[27–29] By contrast, trions, which are three-body charged excitonic bound states of electrons and holes, are expected to exhibit a much longer valley lifetime compared to excitons;[30–32] thus, they could potentially function as an alternative information carrier in optovalleytronics.[30,31] However, trion emission is normally very weak and spatially heterogeneous, which prohibits the realistic application of trions in these materials. Many methods have been used to enhance or increase PL emission efficiency, such as using an *h*-BN substrate or chemical treatment,[3,33–36] and the valley lifetime, such as heterostructure methods.[37,38] Among the available methods, chemical doping using the *p*-type dopant molecule F_4TCNQ is an easy and effective method to modify exciton/trion PL emission properties.[3] However, the effect of F_4TCNQ treatment on the trion valley polarization property at low temperature requires further clarification.

Here, we evaluate the PL and valley polarization characteristics of 1L MoS_2 on a SiO_2/Si substrate before and after the F_4TCNQ treatment. A polarization-resolved PL mapping method was used to investigate the position-dependent PL and valley polarization properties of the whole sample. The results indicated that after the treatment, the average PL intensity at room temperature increased more than 7 times, which is consistent with previous reports.[3] At 15 K, trion PL intensity also increased after the F_4TCNQ treatment. We confirmed that the trion PL intensity enhancement is likely caused by an increase in the trion effective lifetime from $<\sim$20 ps (the lower limit of our detection system) to ~70 ps. Moreover, we found that the spatial uniformity of valley polarization of trions increased compared to the untreated samples, with the average trion valley polarization retained as high as 0.75 after the treatment. The near constant degree of valley optimization with increased trion lifetime suggests a long trion valley lifetime of more than nanoseconds order, which is much longer than the neutral bright exciton valley lifetimes that are in the order of a few tens of picoseconds.[29,31,39] These results highlight the usefulness of bright and highly valley polarized trion PL in F_4TCNQ-treated 1L MoS_2 in optovalleytronics.

1L MoS_2 was prepared using a standard mechanical exfoliation method from the bulk crystal (hq graphene) and then transferred onto a SiO_2/Si substrate.[40] The thickness was first identified using the optical contrast and confirmed using Raman and PL spectroscopy.[41,42] The F_4TCNQ treatment was performed at room temperature in air using a drop cast method.[3] Before and after the F_4TCNQ treatment, PL spectra under excitation using a laser of 532 nm (2.33 eV) were measured using a micro-PL setup (Nanophoton RAMAN-FM). Valley polarization measurements were carried out at a home-built optical setup with an excitation wavelength of 633 nm (1.96 eV), which is near the resonance of A-exciton absorption in 1L MoS_2 at 15 K and is known to yield higher valley polarization of trions than 532 nm (2.33 eV) excitation.[7] The circularly polarized excitation light (σ^+) was obtained by inserting a linear polarizer and a quarter wave plate in front of the objective lens. The schematic of the optical setup is shown in Fig. S1 (supplementary data is available online at stacks.iop.org/APEX/13/035002/mmedia). For the time-correlated single-photon counting method, a Si avalanche photodiode was used as a detector under a pulsed excitation of 580 nm (2.14 eV) light extracted from broadband supercontinuum light (~20 ps in duration and 40 MHz in frequency) using a monochromator and optical filters.

Figure 1(a) shows the sample image of 1L MoS_2 under the optical microscope. The PL spectra before and after the treatment under excitation using a 532 nm laser are shown in

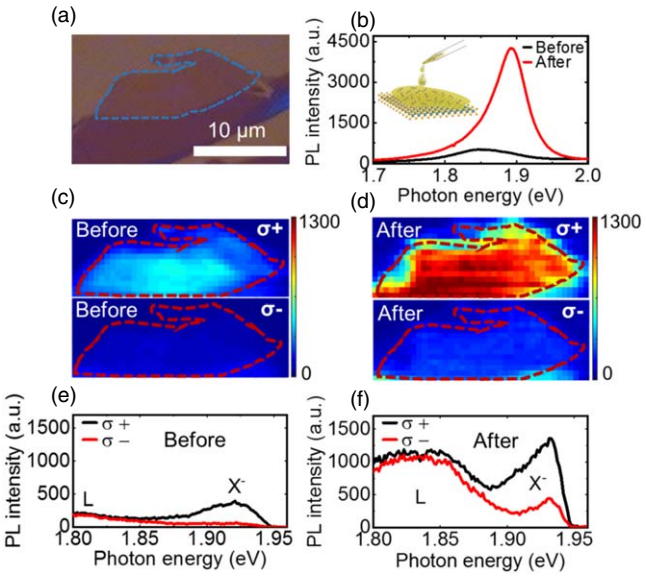

Fig. 1. (Color online) (a) Optical image of 1L MoS_2 on a SiO_2/Si substrate. (b) PL spectra of 1L MoS_2 before and after the treatment at 300 K excited using a 532 nm (2.33 eV) laser, and inset is the schematic of F_4TCNQ treatment using a drop cast method. (c) and (d): PL intensity maps from σ^+ and σ^- circularly polarized trion emissions before and after the treatment. The blue (a) and red (c, d) dashed line area indicates the monolayer part. (e) and (f): PL spectra before and after treatment. L and X^- are the localized state and trion peaks, respectively.

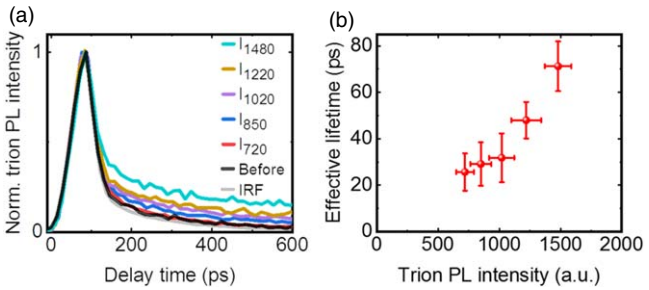

Fig. 2. (Color online) (a) Time-resolved PL decay profile of trions at points with various trion PL intensities I_α, where α is the corresponding PL intensity (in arb. units), comparing with the PL decay profile before the treatment (Black). (b) Effective PL lifetime of trions at various points plotted as a function of the corresponding trion PL intensity.

Fig. 1(b). After the treatment, the PL intensity of the sample at room temperature increased by more than 7 times of the as-prepared sample. The PL spectral peak energy showed a blue shift; this shift has been attributed to the modification of the exciton (X) and trion (X^-) intensity ratio because of carrier (electron) extraction from the naturally heavy *n*-doped 1L MoS_2.[3] The fitted results (Fig. S2 in supplementary data) indicate that the intensity ratio of the exciton (at ~1.89 eV) and trion (at ~1.85 eV), I_X/I_X^-, increased by 50 times after the treatment.

To evaluate the PL and valley polarization properties of trions at low temperature, a 633 nm (1.96 eV) He–Ne laser was used for near A-exciton resonant excitation of the sample; this excitation condition is known to yield high trion valley polarization.[7,18,43,44] Figures 1(c) and 1(d) show the σ^+ and σ^- trion PL intensity maps obtained from more than 700 mapping points under the σ^+ circularly polarized excitation at 15 K before and after the treatment, respectively. After treatment, the trion PL intensity distinctly increased and the spatial uniformity of the PL intensity showed minor improvement. The typical PL spectra in Figs. 1(e) and 1(f) showed the localized state (L) and trion PL (X^-) features. The exciton peaks were cut by the edge filter because of the use of a laser wavelength near-resonant to the A-excitons (1.96 eV).

To understand the origin of the enhanced trion PL intensity, time-resolved PL measurements before and after the treatment were also carried out. As shown in Fig. 2(a), before the treatment, the typical time-resolved PL decay profile is almost same with the instrumental response function (IRF), which implies that the decay time is shorter than the temporal resolution of our measurement system. After the treatment, the average PL decay time considerably increased. This result suggests that the increased trion PL intensity is likely caused by the increased nonradiative lifetime of trions, which could be attributed to the S vacancy defect (that may function as a nonradiative center) passivated by the molecular absorption,[35,45–47] or reduced nonradiative decay pathways of trions owing to reduced carrier-trion scattering.[48–50]

It is noticed that time-resolved PL decay profile/PL intensity in the sample exhibited a position-dependent property as shown in Figs. 1(d) and 2(a). A longer PL decay time was observed at the higher trion PL intensity point [Fig. 2(a)]. To further address the origin of the position-dependent trion PL intensity, effective lifetime $\langle\tau_{tr}\rangle$ of bright trions was evaluated at various positions on the treated sample. $\langle\tau_{tr}\rangle$ was obtained via time-resolved PL decay curve fitting using convolutions of the biexponential function $I(t) = C_1 \exp(-t/\tau_1) + C_2 \exp(-t/\tau_2)$ and the IRF, which was then calculated as $\langle\tau_{tr}\rangle = (C_1\tau_1 + C_2\tau_2)/(C_1 + C_2)$. As shown in Fig. 2(b), the results showed that the $\langle\tau_{tr}\rangle$ considerably increased up to ~70 ps after the F_4TCNQ treatment, and a strong positive correlation between the effective trion PL lifetime $\langle\tau_{tr}\rangle$ and the trion PL intensity was observed. This result also supports the argument that the trion PL lifetime is dominated by nonradiative relaxation pathways of trions, and the spatial variation in the local defect density or in the condition of passivation is the cause of spatial heterogeneity in the trion PL intensity of the sample.

To compare the trion valley polarization ρ_{tr} throughout the sample, the valley polarization map was obtained using σ^+ and σ^- polarized PL spectra at all the measured points as shown in Fig. 3(a). The ρ_{tr} was calculated using the relation $\rho_{tr} = (I_+ - I_-)/(I_+ + I_-)$, where I_+ and I_- are the trion PL intensity with σ^+ and σ^- polarization, respectively. After the treatment, spatial uniformity of the valley polarization increased with the exception of the sample edge points which were affected by numerous factors, such as residual strain, folding, insufficient substrate contacts, and insufficient excitation.[51–55] The valley polarizations at all points excluding the sample edges were plotted as a function of the corresponding trion PL intensity in Fig. 3(b); however, no considerable change of valley polarization was observed with variation of the PL intensity. These results showed that the F_4TCNQ chemical doping treatment only affects the trion PL intensity, and does not increase or decrease the degree of valley polarization of trions.

To further understand this PL intensity-independent valley polarization of trions, valley polarizations at various points

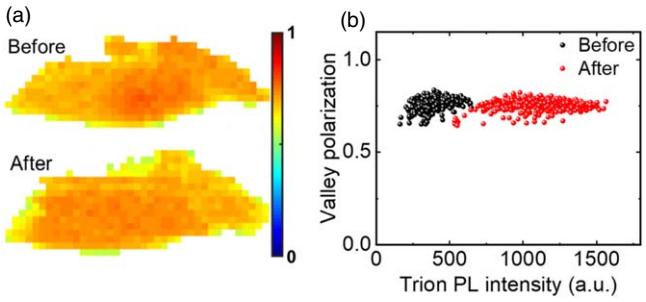

Fig. 3. (Color online) (a) Valley polarization map of trions in 1L MoS_2 before and after the F_4TCNQ treatment at 15 K. (b) Valley polarization as a function of trion PL intensity at various spots before and after the treatment.

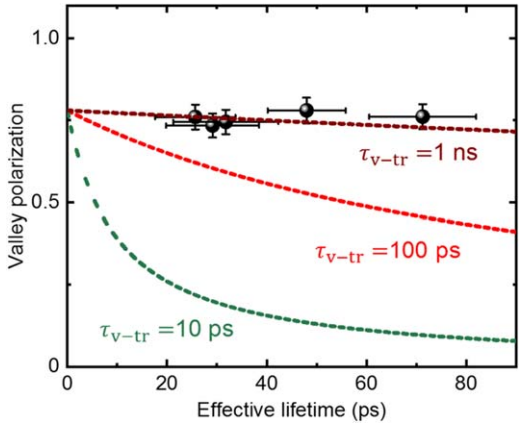

Fig. 4. (Color online) Trion valley polarization of F_4TCNQ-treated 1L MoS_2 at various positions as a function of the corresponding effective lifetime. The dashed curves are simulated based on Eq. (1) with various τ_{v-tr} values.

on the sample were plotted as a function of the corresponding effective trion PL lifetimes in Fig. 4, and the results observed were similar to those in Fig. 3(b); uniform trion valley polarization was obtained regardless of the trion effective lifetimes $\langle\tau_{tr}\rangle$ at each point. Under the direct excitation of A-excitons and successive trion generation by carrier capture of the excitons, the steady-state trion valley polarization can be phenomenologically expressed as

$$\rho_{tr} = \frac{1}{1 + \langle\tau_{tr}\rangle/\tau_{v-tr}}\rho_{ex}, \quad (1)$$

where $\langle\tau_{tr}\rangle$, τ_{v-tr}, and ρ_x are effective trion lifetime, trion valley lifetime, and initially created exciton valley polarization, respectively.[6,7,56] The Eq. (1) suggests that $\langle\tau_{tr}\rangle$ and ρ_{tr} are correlated in principle.

Interestingly, these observed trends are considerably different from cases involving neutral bright excitons. The extended bright exciton lifetime causes a strong reduction in the steady-state exciton valley polarization because the electron-hole exchange interaction dominates valley relaxation with a time scale of picoseconds, which is much shorter than or is at most comparable to the exciton lifetime in 1L TMDs.[7,21,29] According to Eq. (1), the correlation of $\langle\tau_{tr}\rangle/\tau_{v-tr}$ was simulated and plotted as dashed curves in Fig. 4, where the ρ_{ex} was estimated as 0.8. From the comparison of the experimental data with the simulated curves, $\langle\tau_{tr}\rangle/\tau_{v-tr} \ll 1$ was deduced, which implied that the trion valley relaxation time τ_{v-tr} was much longer than $\langle\tau_{tr}\rangle$. Considering the maximum $\langle\tau_{tr}\rangle$ is in the order of ~70 ps, τ_{v-tr} should be in the order of nanoseconds at minimum, which is consistent with previously reported results.[39,57,58] This long valley lifetime of trions may be attributed to many reasons: suppressed electron-hole exchange effect in three-body trions compared with excitons, chemical adsorption-induced change in the screening effect of Coulomb interactions, and/or reduced scattering due to passivation of charged vacancy defects. The long trion valley lifetime, τ_{v-tr}, is a manifestation of the lack of an efficient intrinsic valley relaxation mechanism for trions at low temperatures,[32] which results in a high valley polarization of trions that is insensitive to the local fluctuations in $\langle\tau_{tr}\rangle$. Thus, the spatial uniformity of valley polarization can be kept high, despite $\langle\tau_{tr}\rangle$ increasing several times after the F_4TCNQ treatment.

Acknowledgments We thank Yan Zhang, Masafumi Shimasaki, and Taishi Nishihara for helpful discussions. This research was supported by JSPS KAKENHI Grant Numbers JP16H00911, JP15K13337, JP15H05408, JP15K13500, JP16H00910, JP16H06331, JP17K19055, JP17H06786, JP19K14633 by the Asahi Glass Foundation, by JST CREST (JPMJCR16F3, JPMJCR18I5), and by the Research Foundation for Opto-Science and Technology.

ORCID iDs Yuhei Miyauchi https://orcid.org/0000-0002-0945-0265

1) A. Splendiani, L. Sun, Y. Zhang, T. Li, J. Kim, C. Y. Chim, G. Galli, and F. Wang, Nano Lett. **10**, 1271 (2010).
2) K. F. Mak, C. Lee, J. Hone, J. Shan, and T. F. Heinz, Phys. Rev. Lett. **105**, 136805 (2010).
3) S. Mouri, Y. Miyauchi, and K. Matsuda, Nano Lett. **13**, 5944 (2013).
4) J. S. Ross et al., Nat. Commun. **4**, 1474 (2013).
5) H. Zeng, B. Zhu, K. Liu, J. Fan, X. Cui, and Q. M. Zhang, Phys. Rev. B **86**, 241301 (2012).
6) T. Cao et al., Nat. Commun. **3**, 887 (2012).
7) K. F. Mak, K. He, J. Shan, and T. F. Heinz, Nat. Nanotechnol. **7**, 494 (2012).
8) D. Xiao, G. Bin Liu, W. Feng, X. Xu, and W. Yao, Phys. Rev. Lett. **108**, 196802 (2012).
9) J. R. Schaibley, H. Yu, G. Clark, P. Rivera, J. S. Ross, K. L. Seyler, W. Yao, and X. Xu, Nat. Rev. Mater. **1**, 16055 (2016).
10) K. F. Mak and J. Shan, Nat. Photonics **10**, 216 (2016).
11) T. Cai, S. A. Yang, X. Li, F. Zhang, J. Shi, W. Yao, and Q. Niu, Phys. Rev. B **88**, 115140 (2013).
12) G. Aivazian, Z. Gong, A. M. Jones, R. L. Chu, J. Yan, D. G. Mandrus, C. Zhang, D. Cobden, W. Yao, and X. Xu, Nat. Phys. **11**, 148 (2015).
13) A. Srivastava, M. Sidler, A. V. Allain, D. S. Lembke, A. Kis, and A. Imamoglu, Nat. Phys. **11**, 141 (2015).
14) P. Back, M. Sidler, O. Cotlet, A. Srivastava, N. Takemura, M. Kroner, and A. Imamoğlu, Phys. Rev. Lett. **118**, 237404 (2017).
15) A. M. Jones, H. Yu, J. R. Schaibley, J. Yan, D. G. Mandrus, T. Taniguchi, K. Watanabe, H. Dery, W. Yao, and X. Xu, Nat. Phys. **12**, 323 (2016).
16) M. Manca et al., Nat. Commun. **8**, 14927 (2017).
17) A. M. Jones et al., Nat. Nanotechnol. **8**, 634 (2013).
18) D. Lagarde, L. Bouet, X. Marie, C. R. Zhu, B. L. Liu, T. Amand, P. H. Tan, and B. Urbaszek, Phys. Rev. Lett. **112**, 047401 (2014).
19) Z. Li, R. Ye, R. Feng, Y. Kang, X. Zhu, J. M. Tour, and Z. Fang, Adv. Mater. **27**, 5235 (2015).
20) S. Konabe, Appl. Phys. Lett. **109**, 073104 (2016).
21) Y. Miyauchi et al., Nat. Commun. **9**, 2598 (2018).
22) K. Shinokita, X. Wang, Y. Miyauchi, K. Watanabe, T. Taniguchi, and K. Matsuda, Adv. Funct. Mater. **29**, 1900260 (2019).
23) P. Rivera, K. L. Seyler, H. Yu, J. R. Schaibley, J. Yan, D. G. Mandrus, W. Yao, and X. Xu, Science **351**, 688 (2016).
24) O. L. Sanchez, D. Ovchinnikov, S. Misra, A. Allain, and A. Kis, Nano Lett. **16**, 5792 (2016).
25) D. Zhong et al., Sci. Adv. **3**, e1603113 (2017).
26) W.-T. Hsu et al., Nat. Commun. **9**, 1356 (2018).
27) C. Mai, A. Barrette, Y. Yu, Y. G. Semenov, K. W. Kim, L. Cao, and K. Gundogdu, Nano Lett. **14**, 202 (2014).
28) C. Mai, Y. G. Semenov, A. Barrette, Y. Yu, Z. Jin, L. Cao, K. W. Kim, and K. Gundogdu, Phys. Rev. B **90**, 041414 (2014).

29) C. R. Zhu, K. Zhang, M. Glazov, B. Urbaszek, T. Amand, Z. W. Ji, B. L. Liu, and X. Marie, Phys. Rev. B **90**, 161302 (2014).
30) G. Wang, L. Bouet, D. Lagarde, M. Vidal, A. Balocchi, T. Amand, X. Marie, and B. Urbaszek, Phys. Rev. B **90**, 075413 (2014).
31) A. Singh et al., Phys. Rev. Lett. **117**, 257402 (2016).
32) K. Shinokita, X. Wang, Y. Miyauchi, K. Watanabe, T. Taniguchi, S. Konabe, and K. Matsuda, Phys. Rev. B **99**, 245307 (2019).
33) Y. Hoshi, T. Kuroda, M. Okada, R. Moriya, S. Masubuchi, K. Watanabe, T. Taniguchi, R. Kitaura, and T. Machida, Phys. Rev. B **95**, 241403 (2017).
34) X. Zhang et al., ACS Nano **13**, 3341 (2019).
35) S. Tongay, J. Zhou, C. Ataca, J. Liu, J. S. Kang, T. S. Matthews, L. You, J. Li, J. C. Grossman, and J. Wu, Nano Lett. **13**, 2831 (2013).
36) M. Amani et al., Science **350**, 1065 (2015).
37) P. Rivera et al., Nat. Commun. **6**, 6242 (2015).
38) J. Kim et al., Sci. Adv. **3**, e1700518 (2017).
39) G. Plechinger, P. Nagler, A. Arora, R. Schmidt, A. Chernikov, A. G. Del Águila, P. C. M. Christianen, R. Bratschitsch, C. Schüller, and T. Korn, Nat. Commun. **7**, 12715 (2016).
40) K. S. Novoselov, A. K. Geim, S. V. Morozov, D. Jiang, Y. Zhang, S. V. Dubonos, I. V. Grigorieva, and A. A. Firsov, Science **306**, 666 (2004).
41) C. Lee, H. Yan, L. E. Brus, T. F. Heinz, J. Hone, and S. Ryu, ACS Nano **4**, 2695 (2010).
42) S. L. Li, H. Miyazaki, H. Song, H. Kuramochi, S. Nakaharai, and K. Tsukagoshi, ACS Nano **6**, 7381 (2012).
43) H. Zeng, J. Dai, W. Yao, D. Xiao, and X. Cui, Nat. Nanotechnol. **7**, 490 (2012).
44) G. Sallen et al., Phys. Rev. B **86**, 081301 (2012).
45) D. Kiriya, M. Tosun, P. Zhao, J. S. Kang, and A. Javey, J. Am. Chem. Soc. **136**, 7853 (2014).
46) H. Nan et al., ACS Nano **8**, 5738 (2014).
47) H. Wang, C. Zhang, and F. Rana, Nano Lett. **15**, 339 (2015).
48) E. Liu, J. van Baren, Z. Lu, M. M. Altaiary, T. Taniguchi, K. Watanabe, D. Smirnov, and C. H. Lui, Phys. Rev. Lett. **123**, 027401 (2019).
49) D. K. Efimkin and A. H. MacDonald, Phys. Rev. B **95**, 035417 (2017).
50) D. Van Tuan, B. Scharf, Z. Wang, J. Shan, K. F. Mak, I. Žutić, and H. Dery, Phys. Rev. B **99**, 085301 (2019).
51) A. Castellanos-Gomez, R. Roldán, E. Cappelluti, M. Buscema, F. Guinea, H. S. J. Van Der Zant, and G. A. Steele, Nano Lett. **13**, 5361 (2013).
52) C. R. Zhu et al., Phys. Rev. B **88**, 121301 (2013).
53) N. D. Kay, B. J. Robinson, V. I. Fal'Ko, K. S. Novoselov, and O. V. Kolosov, Nano Lett. **14**, 3400 (2014).
54) M. Buscema, G. A. Steele, H. S. J. van der Zant, and A. Castellanos-Gomez, Nano Res. **7**, 561 (2014).
55) Y. Kwon, K. Kim, W. Kim, S. Ryu, and H. Cheong, Curr. Appl. Phys. **18**, 941 (2018).
56) G. Kioseoglou, A. T. Hanbicki, M. Currie, A. L. Friedman, D. Gunlycke, and B. T. Jonker, Appl. Phys. Lett. **101**, 221907 (2012).
57) L. Yang, N. A. Sinitsyn, W. Chen, J. Yuan, J. Zhang, J. Lou, and S. A. Crooker, Nat. Phys. **11**, 830 (2015).
58) E. J. McCormick, M. J. Newburger, Y. K. Luo, K. M. McCreary, S. Singh, I. B. Martin, E. J. Cichewicz, B. T. Jonker, and R. K. Kawakami, 2D Mater. **5**, 011010 (2017).